RESEARCH

Modeling Canopy Carbon and Water Fluxes Using a Multilayered Model over a Temperate Meadow in Inner Mongolia

Nina Chen[1] · Anzhi Wang[2] · Juan An[3] · Yushu Zhang[1] · Ruipeng Ji[1] · Qingyu Jia[1] · Ziqi Zhao[1] · Dexin Guan[2]

Abstract

To incorporate canopy vertical structure in a process-based model over a temperate meadow, a multilayered model estimated canopy carbon flux (F_c) and water flux (LE) was applied by comparing with eddy covariance measurements in Inner Mongolia, China. Simulations of diurnal, seasonal CO_2 and H_2O fluxes and model sensitivity to parameters and variables were analyzed. The results showed that the model underestimated F_c and LE by about 0.6% and 5.0%, respectively. It was able to simulate the diurnal and seasonal variation of F_c and LE and performed well during the day and in the growing season, but poorly at night and early in the growing season. F_c was more sensitive to the leaf nitrogen content distribution coefficient and maximum catalytic activity of Rubisco, whereas LE showed greater sensitivity to the stomatal conductance parameter a_1, empirical coefficient of stomatal response to saturated vapor pressure difference V_{pds0}, and minimum stomatal conductance of CO_2 g_{sc0}. The response of F_c to environmental factors was ranked as air CO_2 concentration (C_a) > air temperature (T_a) > photosynthetically active radiation (PAR) > soil water content (θ_{sm}) > vapor pressure deficit (VPD) > wind speed (u_0). The response of LE to environmental factors was ranked as T_a > VPD > θ_{sm} > PAR > C_a > u_0. The response of LE to vegetation characteristic parameters was greater than that of F_c.

Keywords Carbon and water exchange · Ecological modeling · Eddy covariance · Multilayered model · Sensitivity analysis

Introduction

Exchange of carbon and water fluxes between the atmosphere and vegetation depend on complex and non-linear interplay among physiological, ecological, biochemical, and edaphic factors and meteorological conditions (Huang et al. 2016; He et al. 2017; Fell et al. 2018). Direct observation of many variables associated with energy transfer and material circulation is difficult on a large scale. The most common models for estimation of carbon and water fluxes are statistical models (Shen et al. 2011) and comprehensive process-based coupled carbon and water models (Leuning et al. 1995; Wang and Leuning 1998). The advantages of a statistical model are that it is simple in form and easy to derive. But it is more empirical and difficult to extrapolate to other regions. The physical interpretation is unclear and a statistical model lacks predictive power. A process-based carbon and water flux coupling model has a clear mechanism. The combination of plant physiological characteristics, canopy structure, soil characteristics, and climatic variables has a certain theoretical basis and clear physical meaning. Such a model not only simulates carbon and water fluxes at the single-leaf scale (Yu et al. 1998), but can be extended to canopy (Sellers et al. 1992) and ecosystem scales (Leuning et al. 1995; Wang and Leuning 1998), and even to regional scales (McMurtrie et al. 1992) and some global climate models (Sellers et al. 1996).

Process-based coupled carbon and water flux models are based on soil–plant–vegetation–atmosphere transfer interactions and include big-leaf, two-leaf, and multilayered models. A multilayered model considers parameters measured

✉ Dexin Guan
251926732@qq.com; dxguan@iae.ac.cn

1 Liaoning Provincial Key Laboratory of Agricultural Meteorological Disasters, Institute of Atmospheric Environment, China Meteorological Administration, Shenyang 110166, China

2 State Key Laboratory of Forest and Soil Ecology, Institute of Applied Ecology, Chinese Academy of Sciences, Shenyang 110016, China

3 Shandong Provincial Key Laboratory of Water and Soil Conservation and Environmental Protection, College of Resources and Environment, Linyi University, Linyi 276000, China

at the leaf scale and the spatial distribution of vegetation physiological parameters as well as climatic variables, and integrates the fluxes of each layer to derive the total fluxes. Thus, a multilayered model is considered to be reasonable and has been employed in many studies (Leuning et al. 1995; Shi et al. 2010; Qu and Zhao 2016).

Mongolian grasslands are sensitive to climate change and human activities. The Mongolian steppe is located between Siberian coniferous forest and the Asian Gobi Desert. Significant changes in temperature, precipitation, and other climatic variables, and increased grassland degradation and desertification are predicted for the future (IPCC 2001). Meadow, the most productive type of grassland supporting livestock production, is located in the eastern part of Inner Mongolia (Liao and Jia 1996). Meadow steppe constitutes 11% of the 7.88×10^5 km^2 of native grassland in Inner Mongolia (Han et al. 2008). Approximately 80% of the plant biomass in meadow steppe is composed of *Phragmites australis*, *Leymus chinensis*, *Glycine soja*, *Plantago asiatica*, and *Ranunculus microphyllus*. Extensive variability in photosynthetic parameters of these species lead to differences in photosynthesis productivity (Wullschleger 1993; Chen et al. 2014), thus influencing the carbon and water exchange of grassland ecosystems. In addition, each species occupies a different height within the canopy and hence shows a different competitive ability for solar radiation (Xue et al. 2017; Zhao et al. 2018). Consequently, canopy vertical structure is more difficult to incorporate in a carbon and water fluxes model for meadow (Chang et al. 2018). The majority of previous studies focused on vegetation composed of a single species (Leuning 1995) or vegetation types other than grassland (Kucharik et al. 2006; Shi et al. 2010). To the best of our knowledge, no previous study has modeled canopy carbon and water fluxes for a mixed-species meadow.

In this paper, a multilayered model estimated canopy carbon and water fluxes was applied over a temperate meadow. It was tested by comparing simulated CO_2 and H_2O fluxes with eddy covariance measurements across half-hour to three-year time scales firstly. And then, the sensitivity of the model to physiological, environmental, and vegetation characteristic parameters were analyzed.

Materials and Methods

Model Description

The model used in this paper was developed by Leuning et al. (1995), tested on a wheat crop canopy by Leuning et al. (1998), and revised for a mixed forest by Shi et al. (2010). The multilayered model at the canopy scale included four components: radiation absorption, coupling of a single-leaf

stomatal conductance-energy balance-photosynthetic model, spatial distribution of physiological parameters, and integration of space and time.

In this paper, the canopy radiation absorption, coupling of a single-leaf stomatal conductance-energy balance-photosynthetic model, and spatial distribution of physiological parameters were similar to those of the previous studies (Leuning et al. 1995; Shi et al. 2010), whereas the integration of space and time was revised to be compatible with meadow steppe vegetation.

Canopy Radiation Absorption

Radiation absorbed by sunlit leaves (Q_{sl}) is expressed as (Leuning et al. 1995):

$$Q_{sl}(\xi) = Q_{lb} + Q_{sh}(\xi) \tag{1}$$

where ξ is the cumulative leaf area index measured from the top of the canopy downwards, Q_{lb} is the diffuse radiation absorbed by all leaves at canopy depth ξ, and Q_{sh} is the radiation absorbed by shaded leaves.

Q_{sh} is estimated by the formula:

$$Q_{sh}(\xi) = Q'_{ld}(\xi) + Q_{lbs}(\xi) \tag{2}$$

where Q'_{ld} and Q_{lbs} are the absorbed components of incoming diffuse and scattered beam radiation, respectively, and are associated with the extinction coefficient for radiation and the leaf area index (Goudriaan and van Laar 1994).

Coupling of Single-Leaf Stomatal Conductance-Energy Balance–Photosynthetic Model

Stomatal and Boundary Layer Conductance Model Total conductance of CO_2 (g_{tc}) and H_2O (g_{tw}) from the substomatal cavities to the air outside the leaf boundary layer are calculated as:

$$g_{tc} = \frac{1}{1/g_{sc} + 1/g_{bc}} \tag{3}$$

$$g_{tw} = \frac{1}{1/g_{sw} + 1/g_{bw}} \tag{4}$$

The stomatal conductance of CO_2 (g_{sc}) is calculated as (Leuning 1995):

$$g_{sc} = g_{sc0} + \frac{a_1 \cdot f_{sm} \cdot A_n}{(C_s - \Gamma^*) \cdot (1 + Vpd_s/Vpd_{s0})} \tag{5}$$

where A_n is the CO_2 assimilation rate, g_{sc0} is the minimum stomatal conductance of CO_2 when $A_n = 0$ at the light compensation point, C_s is the CO_2 concentration, Γ^* is the CO_2 compensation point, and the parameter a_1 is associated

with the intercellular CO_2 concentration (C_i) at saturating irradiance as determined by the relationship $1/a_1 = 1 - C_i/C_s$ (Leuning et al. 1995). The function f_{sm} reflects the soil moisture limit (θ_{sm}) on stomatal conductance (Stewart and Verma 1992), Vpd_s is the vapor pressure saturation deficit, and Vpd_{s0} is the empirical coefficient of stomatal response to saturated vapor pressure difference.

The boundary layer conductance of CO_2 (g_{bc}) is proportional to the boundary layer conductance of water vapor (g_{bw}) as:

$$g_{bc} = g_{bw}/(1.37 \cdot m) \tag{6}$$

where the constant 1.37 is the ratio of diffusivity of CO_2 and water vapor in the boundary layer (Von Caemmerer and Farquhar 1981), and m is the molar volume of gas that is required to convert g_{bc} from velocity to molar units.

The boundary layer conductance of water vapor (g_{bw}) is associated with its thickness and the molar diffusivity of water vapor (D_w) in air:

$$g_{bw} = D_w/B_t \tag{7}$$

where B_t is the boundary layer thickness (Aphalo and Jarvis 1993). D_w is calculated as described by Amthor (1994) from the air temperature (T_a).

The stomatal conductance of H_2O (g_{sw}) is calculated as (Leuning 1995):

$$g_{sw} = 1.56 \cdot g_{sc} \cdot m \tag{8}$$

where the constant 1.56 is the ratio of molecular diffusivity for water vapor and CO_2 in air (Leuning et al. 1995).

Leaf Energy-Balance Model

Net radiation absorbed by the leaves is divided into sensible and latent heat. The Penman–Monteith equation is used to calculate latent heat (Leuning et al. 1995), whereas the sensible heat is calculated by the energy-balance model:

$$LE = \frac{s \cdot Y \cdot R_n^* + \rho_a \cdot c_p \cdot Vpd_a \cdot g_{bh}}{s \cdot Y + \gamma \cdot g_{bh}/g_{tw}} \tag{9}$$

$$H = Y \cdot (R_n^* - LE) \tag{10}$$

where R_n^* is the net isothermal radiation absorbed by the leaf, Y is a coefficient associated with radiation conductance (Leuning et al. 1995), LE and H are the latent and sensible heat exchanges between a leaf and its surroundings, respectively, ρ_a is the air density, Vpd_a is the vapor pressure saturation deficit in air, and c_p is the specific heat capacity of dry air.

Leaf Photosynthesis Model

Farquhar et al. (1980) presented a biochemical model of photosynthetic carbon assimilation in C_3 plants:

$$A_n = \min\{A_v, A_j\} - R_d \tag{11}$$

where min{ } denotes 'minimum of', A_v is ribulose bisphosphate carboxylase-oxygenase (Rubisco) activity, A_j is the ribulose bisphosphate (RuP_2) regeneration rate allowed by electron transport, and R_d is 'dark respiration' (defined as the CO_2 evolved other than through the photorespiratory pathway). R_d is proportional to the maximum catalytic activity of Rubisco (V_{cmax}), following (Farquhar et al. 1980):

$$R_d = 0.0089 \cdot V_c\text{max} \tag{12}$$

Given that A_n, LE and g_{sc} are not independent, the values of C_i and g_{sc} must be determined in an iterative fashion. The model is operated in accordance with the method of Shi et al. (2010).

Spatial Distribution of Physiological Parameters

In parameterizing multilayered models, physiological and environmental characteristics should change with depth in the canopy, and sunlit and shaded leaves should be treated separately. The distribution of key environmental and plant factors at different canopy depths (ξ), wind speeds (u), and V_{cmax0} are estimated as follows (Leuning et al. 1995):

$$u(\xi) = u_0 \cdot \exp(-k_u \cdot \xi) \tag{13}$$

$$V_c\text{max} = V_{cmtop} \cdot (-k_n \cdot \xi/\xi_t) \tag{14}$$

where u_0 is the wind speed above the top of the canopy, V_{cmtop} is the value of V_{cmax} at $\xi = 0$, ξ_t is the total leaf area index, k_u is the extinction coefficient for wind speed, and k_n is the distribution coefficient for leaf nitrogen.

Integration of Space and Time

To apply the model to a temperate meadow composed of mixed species, we adjusted the method of dividing the canopy into multilayers. The total canopy thickness of the meadow is about 1.2 m based on the results of a field survey in the vicinity of the flux tower (Chen et al. 2014). The canopy is divided into 12 layers based on the vertical distribution of the dominant species.

The photosynthesis rate $A_c(t)$ and transpiration rate $LE_c(t)$ of each layer of the canopy of one species at time t are calculated as:

$$A_c(t) = \sum_{i=1}^{n} [A_{sl}f_{sl} + A_{sh}f_{sh}]X \tag{15}$$

$$LE_c(t) = \sum_{i=1}^{n} \left[LE_{sl}f_{sl} + LE_{sh}f_{sh} \right] X \qquad (16)$$

where A_{sl} and A_{sh} are the assimilation rates of sunlit and shaded leaves, respectively, of each species, f_{sl} and f_{sh} are the fractions of sunlit and shaded leaf areas, LE_{sl} and LE_{sh} are the evapotranspiration rates of sunlit and shaded leaves of each species, $[A_{sl}f_{sl} + A_{sh}f_{sh}]$ is the assimilation rate of one layer, $[LE_{sl}f_{sl} + LE_{sh}f_{sh}]$ is the evapotranspiration rate of one layer, n is the total number of layers (12), X is the proportion of biomass in a layer of a certain species. Finally, $A_c(t)$ and $LE_c(t)$ at each point of the canopy of each species are respectively summed, which is the net photosynthesis rate A_n and the evapotranspiration rate LE_c of the grass canopy at that time point.

Studied Location

The experiment was carried out in a meadow of Horqin Grasslands in Horqinzuoyihou County, eastern Inner Mongolia, China (as shown in Fig. 1). A measurement tower 4 m in height was established at the study site (43°17′37″ N, 122°16′42″ E, 203 m altitude). The site experiences a temperate continental climate, cold and dry in the dormant season, and relatively warm and wet in the growing season. The mean annual precipitation is 378.8 mm, and the annual mean air temperature is 6.2 °C.

Approximately 80% of the plant biomass at the study site was composed of *Phragmites australis*, *Leymus chinensis*, *Glycine soja*, *Plantago asiatica*, and *Ranunculus microphyllus*. The average height of the vegetation was 0.45 m in the mid-growing season from June to August. The grass at the study site is harvested for livestock forage in September. The field is flat and characterized by the Haplumbrepts soil type (USDA Taxonomy). Soil organic matter content is 8–10%, soil depth is 40–100 cm, and soil pH is 8.5–10.5.

Fig. 1 Map of site's location
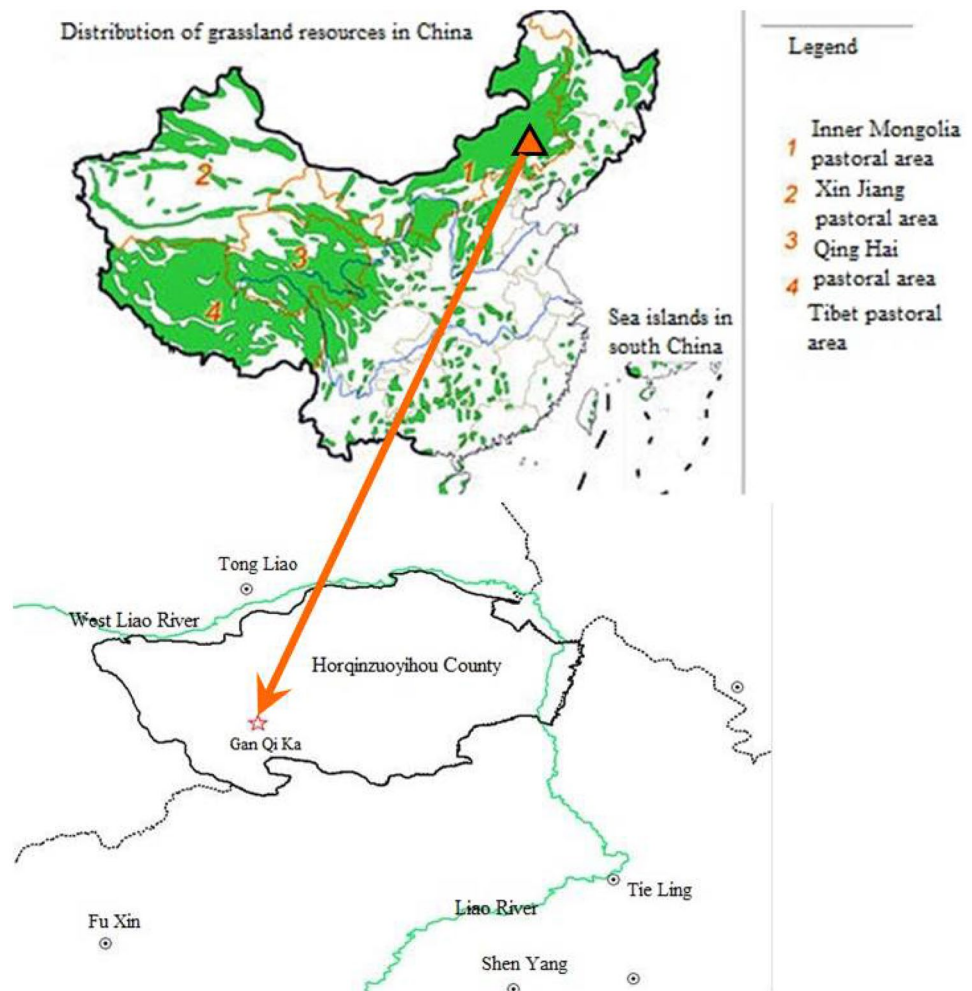
Observed Data Collection

Microclimate and CO$_2$/H$_2$O/Energy Flux Measurements

Eddy covariance and microclimatic instruments were installed on the meteorological tower at the experimental site and have been in operation since August 2007. Eddy covariance, routine meteorological, and solar radiation instruments were installed on the meteorological tower in the meadow. Details of the instrumentation are presented in Table 1. Original signals from the eddy covariance system were sampled at 10 Hz, whereas data from the other instruments were collected at 0.5 Hz. All of the above-mentioned meteorological data were stored as 30-min averages.

Photosynthetic Parameters of Dominant Species

To quantify photosynthetic parameters, such as V_{cmax}, photosynthetic characteristics of the five dominant species were measured in 2010 and 2011 with a LI-6400 portable photosynthesis system (LiCor Inc., Lincoln, NE, USA) equipped with an artificial irradiance source (LiCor 6400-02B red/blue LED light source) and a CO$_2$ concentration source (LiCor 6400-01 CO$_2$ mixer; Chen et al. 2014).

Measurement of Leaf Area Index

Leaf area index was measured by a plant canopy analyzer (LAI-2000, LiCor Inc., Lincoln, NE, USA). The observation site was selected as a cross section of about 200 m long in the southwest of the flux tower, and 12 points were selected before sunrise or after sunset, or on cloudy days. In the early (May) and end (September) growing seasons, the leaf area index is observed every 3–5 days, while every 5–10 days during the mid growing season (June–August).

Measurement of Soil Evaporation

Six small lysimeters (30 cm in height), constructed of PVC, were consisted of outer tubes with diameter of 12 cm and inner tubes with diameter of 10 cm. Lysimeters No. 1, 2, and 3 were placed under the grass canopy, and No. 4, 5, and 6 were placed in a grass-free plot nearby (area 1 m × 2 m, in which the grass was cut every few days to ensure the plot was grass-free). The outer tube was fixed in the soil so that the surface was level with the neighboring soil to avoid damage to the nearby soil structure during operation. When preparing the undisturbed soil, the bottomless lysimeter inner cylinder was vertically pressed into the soil, leaving 0.5 cm of the tube exposed above the soil surface. The inner cylinder containing the undisturbed soil was dug out, and the excess soil at the bottom of the cylinder was excised so that the bottom surface of the cylinder was flat. The bottom surface of the inner cylinder was sealed with a bottom cover with micro holes. The cylinder was weighed at 30-min intervals using a load cell (model 203A, Wuhan Lihe Electric Meter Factory, Wuhan, China). To ensure that the soil moisture content in the lysimeter was similar to that of the surrounding soil, the undisturbed soil in the lysimeter was replaced every 5–7 days.

Calibration Phase

Numerical solution method was used in the process:

Table 1 Introduction of eddy covariance, routine meteorological and solar radiation measurements

Type of measurements	Instrument	Heights
Routine meteorological measurement system		
Air temperature and relative humidity	HMP45C, Vaisala, Helsinki, Finland	1.5 m and 3 m
Precipitation	TE525MM, Campbell Scientific, Inc., USA	1 m
Photosynthetically active radiation	LI190SB, LiCor Inc., USA	1.5 m
Net radiation	NR-LITE, Kipp&Zonen, Delft, Netherlands	1.5 m
Soil moisture	CS616, Campbell Scientific, Inc., USA	5 and 20 cm below ground
Soil temperature	Modell09, Campbell Scientific, Inc., USA	0, 5, 10 and 20 cm below ground
Soil heat flux	HFP01, HukseFlux, Netherlands	5 cm below ground
Eddy covariance system		
Latent heat flux	CSAT3, Campbell Scientific, Inc., USA	3 m
Sensible heat flux	Li-7500, Licor Inc., Nebraska, USA	
Power supply equipment		
Solar panels	T160W, Suntech Power Co. Ltd., China	Surface
Data logger		
Data collector and communication	ModelCR1000, Campbell Scientific, Logan, UT, USA	

1. Give g_{sc} a small initial value, such as 0.1;
2. Simulate the stomatal conductance and boundary layer conductance under the condition of g_{sc}, and obtain the conductance of each resistance segment;
3. Substituting the obtained conductance into the energy balance equations to calculate the leaf temperature (T_l), latent heat flux (LE) and sensible heat flux(H);
4. Substituting the calculated T_l, and a given C_i value into the photosynthesis model, calculate the net photosynthesis rate A_n at this time. Calculate a new C_i value according to the given g_{sc} value and the relationship between A_n and C_i. If the difference between this C_i value and the previously given C_i value is less than a certain smaller critical value (such as 0.01), the model goes to the simulation of stomatal conductance, otherwise repeat the photosynthesis model, until it meets the requirements;
5. Substituting the modeled A_n and C_s into the stomatal conductance model to obtain a new g_{sc}, if the difference between the value and the previously given g_{sc} is less than a certain smaller critical value (such as 0.0001), the model goes to the next period, otherwise repeat Eqs. 2–5, until it meets the requirements.

Evaluation Phase

Model calculated F_c and LE values were compared to the direct observed values using standard statistics and regression analysis. In this paper, we used Mean absolute error (MAE) and root mean squared error (RMSE) as aggregate indicators of model performance. They were computed as:

$$\text{MAE} = \frac{1}{n} \sum_{i=1}^{n} \left| X_{\text{mod},i} - X_{\text{obs},i} \right| \tag{17}$$

$$\text{RMSE} = \sqrt{\frac{1}{n} \sum_{i=1}^{n} \left(X_{\text{mod},i} - X_{\text{obs},i} \right)^2} \tag{18}$$

where $X_{\text{mod},i}$ and $X_{\text{obs},i}$ are the modeled and observed F_c and LE values, respectively for each day i (or 30 min) and n is the sample number.

Simulation Processes

Using the above mentioned multilayered model to simulate the canopy net photosynthesis and evapotranspiration rate from May to August (2010–2011) in Horqin meadow grassland. The time step is 30 min. Using 30 min meteorological data from the meteorological observation tower in Horqin meadow grassland test site as the environmental input variable to calculate the photosynthesis within canopy in the corresponding time, thereby a series of daily

and season changes in photosynthesis obtained. Furthermore, the model sensitivity to parameters and variables were analyzed.

Detailed description is as follows:

1. *Input of environmental factors* Environmental factor data collected every half hour from May 1st to August 30th (2010–2011) (temperature T_a, water vapor pressure e_a, solar radiation S_0, photosynthetically active radiation *PAR*, wind speed u_0, atmospheric pressure P, atmosphere The CO_2 concentration in the C_a) input into the model.
2. *Simulation of radiation absorption* Based on the canopy stratification and the corresponding cumulative leaf area index ξ_t, the solar radiation absorbed by the illuminated and shaded leaves in each layer and the photosynthetically active radiation are calculated.
3. *Simulation of the foliar process* Including photosynthesis model, energy balance equation, stomatal conductance model. Numerical solution method was used in the process as that in the calibration phase described.
4. *Simulation of canopy scale* The A_{sl}, A_{sh}, LE_{sl}, and LE_{sh} of the shaded leaves obtained by the foliar process simulation are substituted into the net photosynthesis calculation formula to obtain the A_n and LE values of a certain layer at that time, and then return to step 2. The simulation of the other layer of the canopy, the final layers are summed, and the total photosynthesis rate A_c and evapotranspiration rate LE_c of the entire canopy at that time are obtained.
5. Daily values of carbon and water fluxes were calculated to analyze the seasonal variation.
6. Model sensitivity analyses when the physiological parameters, environmental factors and vegetation parameters changed.

Model Validation

The canopy CO_2 and H_2O fluxes (A_c and LE_c) used for validation were eddy covariance measurements (A_{eco} and LE_{eco}) minus the soil CO_2 (R_{soil}) and H_2O fluxes (LE_{soil}), respectively.

$$A_{eco} = A_c + R_{soil} \tag{19}$$

$$LE_{eco} = LE_c + LE_{soil} \tag{20}$$

R_{soil} is estimated with consideration of the soil temperature at 0.05 m soil depth (T_s) using an exponential equation:

$$R_{soil} = a3 \cdot \exp\left(b3 \cdot T_s\right) \tag{21}$$

According to Chen et al. (2011), the value of $a3$ is 0.678 and that of $b3$ is 0.106.

Results and Discussion

Verification of the Multilayered Model

Observation data recorded from May to August, 2010 and 2011 in the Korqin meadow were selected to validate the simulation of carbon and water fluxes by the multilayered model. The simulated 30-min values for carbon flux F_c and water flux LE and the observed ones showed good correspondence (Fig. 2). The linear regression line was close to the 1:1 line. The slope, intercept, correlation coefficient, sample number, mean absolute error (MAE), and root mean square error (RMSE) are shown in Table 2. The multilayered model underestimated F_c and LE by about 0.6% and 5.0%, respectively.

The simulation results of the model were not uniform in different days, months, and years. For the different years, F_c was overestimated by 8.6% and underestimated by 4.9%,
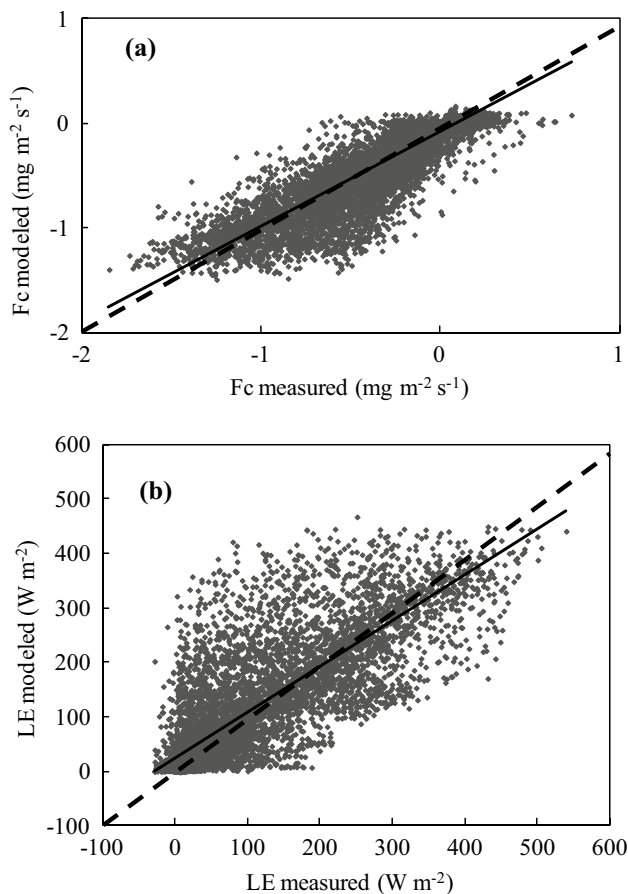
whereas LE was underestimated by 3.1% and 6.6%, in 2010 and 2011, respectively. For different months, F_c was underestimated by 18.8% and overestimated by 1.9%, and LE was underestimated by 34.3% and 1.8%, early in the growing season (May) and during the growing season (June to August), respectively. For daytime (photosynthetically active radiation PAR > 5 μmol m^{-2} s^{-1}), F_c and LE were overestimated by 2.0% and underestimated by 5.8%, respectively.

Simulation of Diurnal Variation of Carbon and Water Fluxes

Simulation of diurnal variation of carbon and water fluxes was analyzed using observation data for three consecutive days per month from May to August in 2011 (Fig. 3). The CO_2 and H_2O fluxes showed distinct diurnal cycles, represented by bell-shaped curves, with low and steady values at night and unimodal distribution of values during the day. The carbon flux was positive at night and negative in the daytime. The ecosystem changed from CO_2 release to absorption after sunrise, and reverted from CO_2 absorption to release before sunset. The maximum net absorption of CO_2 was attained at about 11:30. The water vapor flux was small at night, increased after sunrise, and gradually decreased after sunset. The maximum water vapor flux was attained at around 12:30. Trends for the simulated and observed 30-min values of F_c and LE were essentially identical. Correspondence between the simulated and observed values was superior during the day than at night.

Simulation of Seasonal Variation of Carbon and Water Fluxes

The seasonal variation (Fig. 4) showed that the simulation values for F_c were consistent with the observed values. The total F_c early in the growing season (May) was low, whereas in the growing season (June–August) was much higher. These results are associated with the LAI, leaf physiological activity, and environmental factors such as temperature and radiation. Compared with the observed eddy-covariance values, the simulated values for F_c were higher early in the growing season (May) because leaf physiological activities are poor and the chlorophyll content is lower. The simulation of LE was not reliable, the simulated value was low early in the growing season (May) because the LAI is lower in May and soil evaporation is a large component of LE.

Sensitivity of Multilayered Model to Parameters and Variables

We analyzed sensitivity of multilayered model to the physiological parameters (the parameter a_1, the empirical coefficient of stomatal response to saturated vapor pressure

Fig. 2 Comparison of modeled (Y-axis) against measured (X-axis) 30 min carbon and water flux **a** carbon flux (F_c), and **b** water flux (LE) during May to August, 2010–2011. The solid lines were the best fit linear regressions ($y = ax + b$), and the dashed lines represented 1:1 relation

Table 2 Linear regressions between measured and modeled 30 min carbon and water fluxes and model error estimation

Flux	Process		a	b	R^2	MAE	RMSE	n
Carbon F_c mg m^{-2} s^{-1}	Total		0.911	− 0.082	0.801	0.128	0.194	8799
	Year							
		2010	0.986	− 0.083	0.818	0.133	0.199	3834
		2011	0.861	− 0.080	0.797	0.119	0.190	4965
	Month							
	May		0.732	− 0.034	0.675	0.073	0.109	2702
	June–August		0.889	− 0.120	0.796	0.159	0.224	6097
	Day							
	Daytime		0.84	− 0.141	0.688	0.175	0.235	5696
Water LE W m^{-2}	Total		0.842	23.48	0.672	39.68	65.26	8548
	Year							
		2010	0.836	29.81	0.624	46.37	75.06	3602
		2011	0.843	19.17	0.716	34.81	57.08	4946
	Month							
	May		0.524	18.02	0.368	30.17	51.02	2458
	June–August		0.839	33.01	0.683	43.52	70.20	6090
	Day							
	Daytime		0.753	44.59	0.565	54.72	79.48	5681

a, b and R^2 is the slope, intercept and coefficient of determination, respectively in the regression equation, n the sample number

MAE mean absolute error, *RMSE* root mean squared error

difference Vpd$_{s0}$, the minimum stomatal conductance of CO_2 at the light compensation point g_{sc0}, the leaf nitrogen content distribution coefficient k_n, and maximum Rubisco catalytic activity V_{cmax}), environmental factors (PAR, vapor pressure deficit VPD, wind speed u_0, soil water content θ_{sm}, air temperature T_a, atmospheric CO_2 concentration C_a), and vegetation parameters (leaf area index LAI). The cumulative canopy carbon and water fluxes from May to August with changes in the parameters were shown in Fig. 5. The amplitude of canopy cumulative F_c and LE after changes of parameters is shown in Table 3. The cumulative canopy F_c and LE declined with decrease in the value of a_1, Vpd$_{s0}$, g_{sc0}, PAR and vice versa. But they increased when k_n, V_{cmax} decreased and vice versa. The cumulative F_c and LE decreased concomitant with decrease in temperature. With progressive increase in temperature, the cumulative F_c and LE initially increased but thereafter decreased. VPD had little effect on F_c, but had a greater influence on LE. With a reduction in VPD, cumulative F_c increased and LE decreased, and vice versa. The effect of u_0 on cumulative F_c and LE was small; when the wind speed increased by 10%, the influence on simulated values of F_c and LE was less than 0.1%. C_a had a greater effect on F_c and less impact on LE. The effect of θ_{sm} on F_c and LE was small.

CO_2 flux was most sensitive to k_n and V_{cmax}, whereas water vapor flux was most sensitive to other physiological parameters. The sensitivity of F_c to individual environmental factors was ranked as $C_a > T_a > PAR > \theta_{sm} > VPD > u_0$, whereas the rank order of sensitivity of LE to environmental factors was $T_a > VPD > \theta_{sm} > PAR > C_a > u_0$. The response of LE to vegetation parameters was greater than that of F_c. Overall, the multilayered model could be used to simulate the multi-species meadow canopy productivity under climate change.

Discussion

Common Issues When Simulating Carbon and Water Flux

The multilayered model underestimated F_c and LE by about 0.6% and 5.0%, respectively at meadow site. Similar phenomenon found by some scholars (Shi et al. 2010; Chang et al. 2018; Reed et al. 2018). Underestimations of F_c at meadow site are expected to have resulted from soil respiration which was simply to the exponential relationship of soil temperature. Underestimations of LE are expected to have resulted from canopy evaporation, transpiration, and soil evaporation estimation errors. Systematic measurements on each component of evapotranspiration are essential for the further evaluation and calibration of latent heat flux estimations for vegetated surfaces (Zhang et al. 2016).

The model performed well during the day and in the growing season, but poorly at night and early in the growing season. The reason for this difference is that F_c during
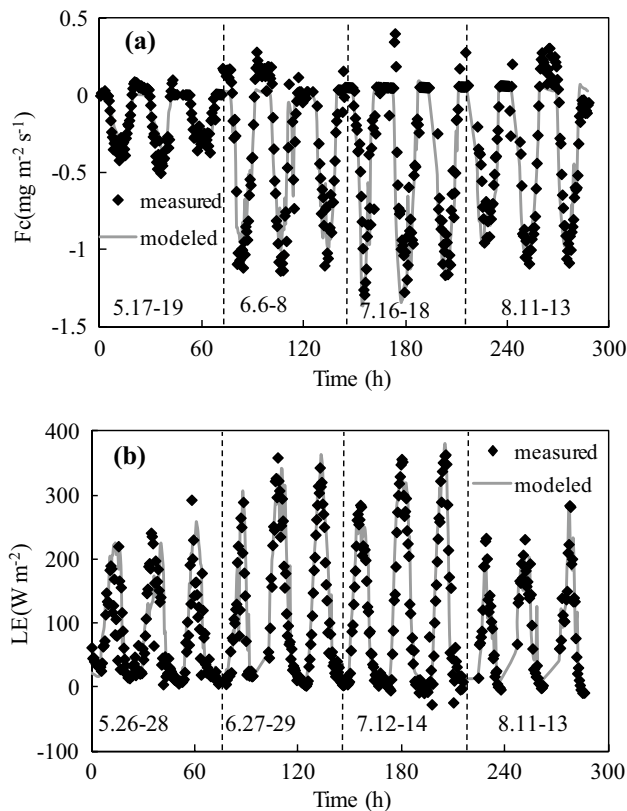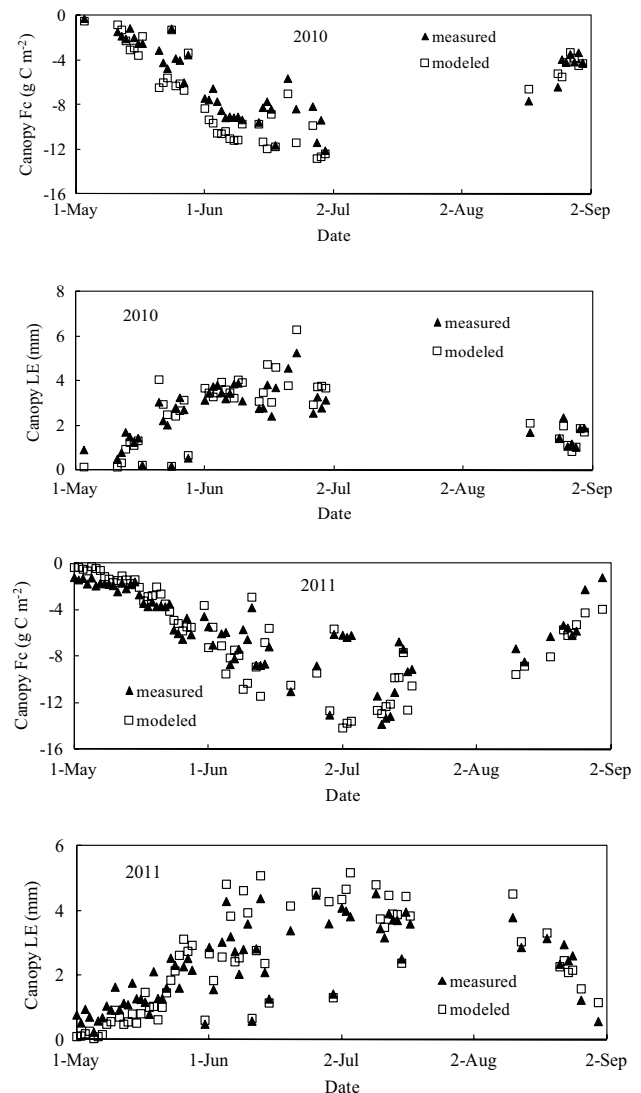
Fig. 3 Comparison of diurnal variation of modeled (line) and measured (dot) canopy carbon and water flux during growing season (May–August, 2011) **a** F_c, **b** LE. 3 days' data in each month were randomly selected

Fig. 4 Seasonal variation of modeled and measured canopy daily carbon and water fluxes for May to August, 2010–2011

the day mainly includes canopy photosynthesis, and vegetation and soil respiration, and canopy photosynthesis activity is much greater than respiration activity. The simulated values for the canopy were similar to the observed values. The F_c at night is mainly from vegetation and soil respiration. Soil respiration is affected by soil moisture content, nutrient concentrations, and soil microbe activities (Huang et al. 2015; Drollinger et al. 2017). The current model does not consider the latter two factors. The low wind speed led to a lower air temperature at the soil surface than at the reference height, resulting in an atmospheric inversion layer, but the model does not account for this temperature difference.

The reason for poor estimation early in the growing season is that physiological and ecological processes in the canopy leaves were mainly considered, but LAI and V_{cmax} at the beginning and end of the growing season each differ substantially, and hence resulted in the deviations in the simulations. Mover, leaf chlorophyll concentration was not measured owing to the limitation of the installed instruments, therefore the impact of chlorophyll content is ignored and the F_c value is small in May. Thus, the percentage error

is relatively large. The reason for the dispersion on LE simulated data is that soil evaporation is a large component of LE. It is not only related to LAI, but also associated with solar radiation, temperature, the saturated vapor pressure difference, wind speed, and other environmental factors. In addition, relatively few leaves have developed in the vegetation in May, and thus the model mainly simulated canopy evaporation and neglected that of the stem. Overall, the multilayered model could be used to simulate the multi-species meadow canopy productivity.

Values of the Parameters of the Model

Simulation of CO_2 and H_2O fluxes affected by values of key input parameters and variables of the model (Liu et al.

Fig. 5 Sensitivity analysis of the multi-layered model for the parameters (take 2011 for example). X-axis was the date, and Y-axis was the canopy cumulative of carbon and water fluxes before and after changes of parameters. The black solid lines were the initial values
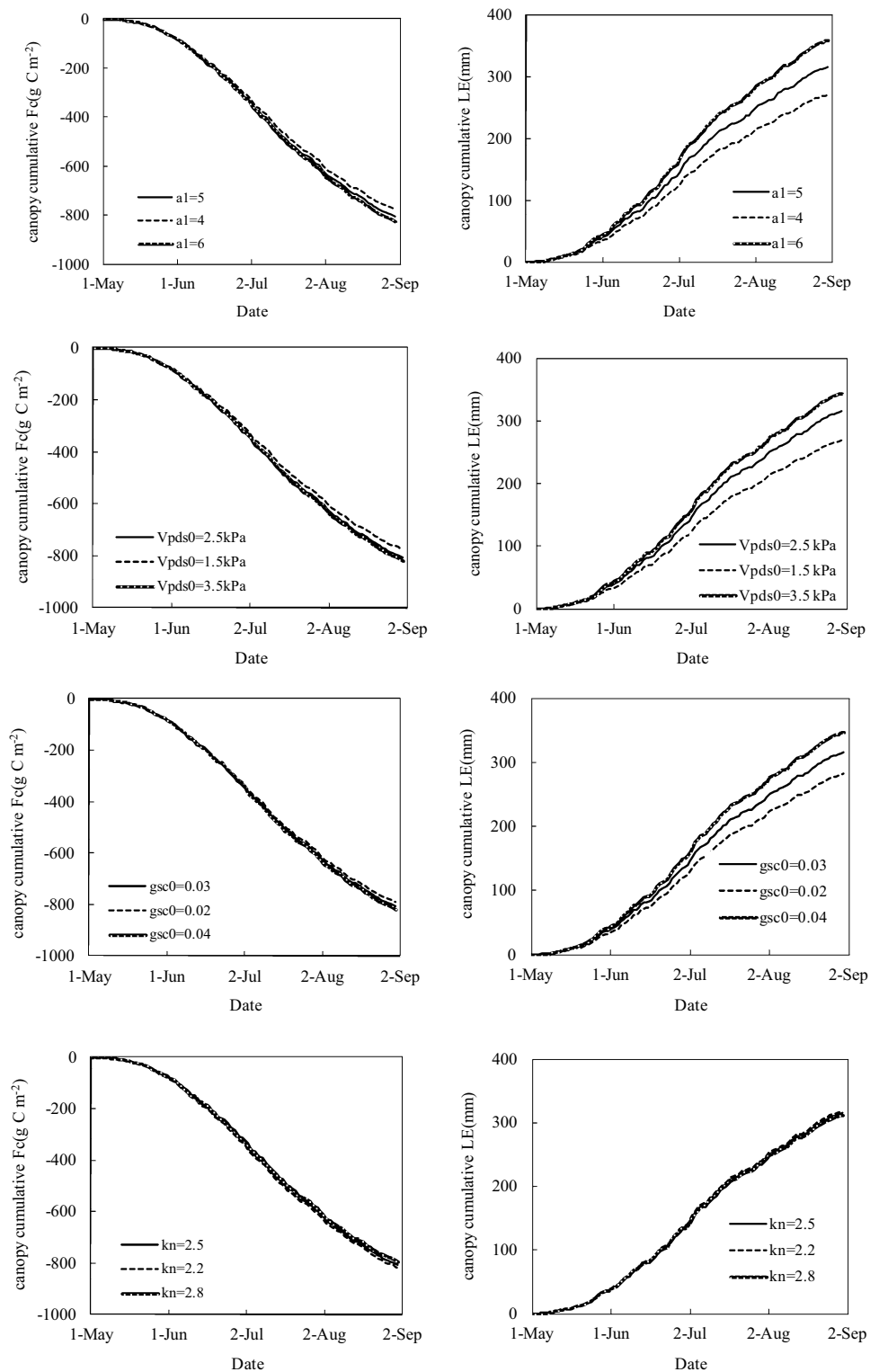
2015). The parameter a_1 is associated with the intercellular CO_2 concentration at light saturation. Leuning et al. (1995) determined in the multilayered model that a_1 ranged in value from 4 to 9 depending on the leaf nitrogen content. Wang and Leuning (1998) reported the a_1 value to be 11 in

a two-leaf model. The empirical coefficient Vpd_{s0} reflects the sensitivity of leaf stomatal conductance to the surface saturated vapor pressure difference Vpd_s. Leuning et al. (1995) determined the Vpd_{s0} value to be 1.5–3.5 kPa. Harley et al. (1992) reported the value of g_{sc0} to be 0.03–0.05 mol

Fig. 5 (continued)
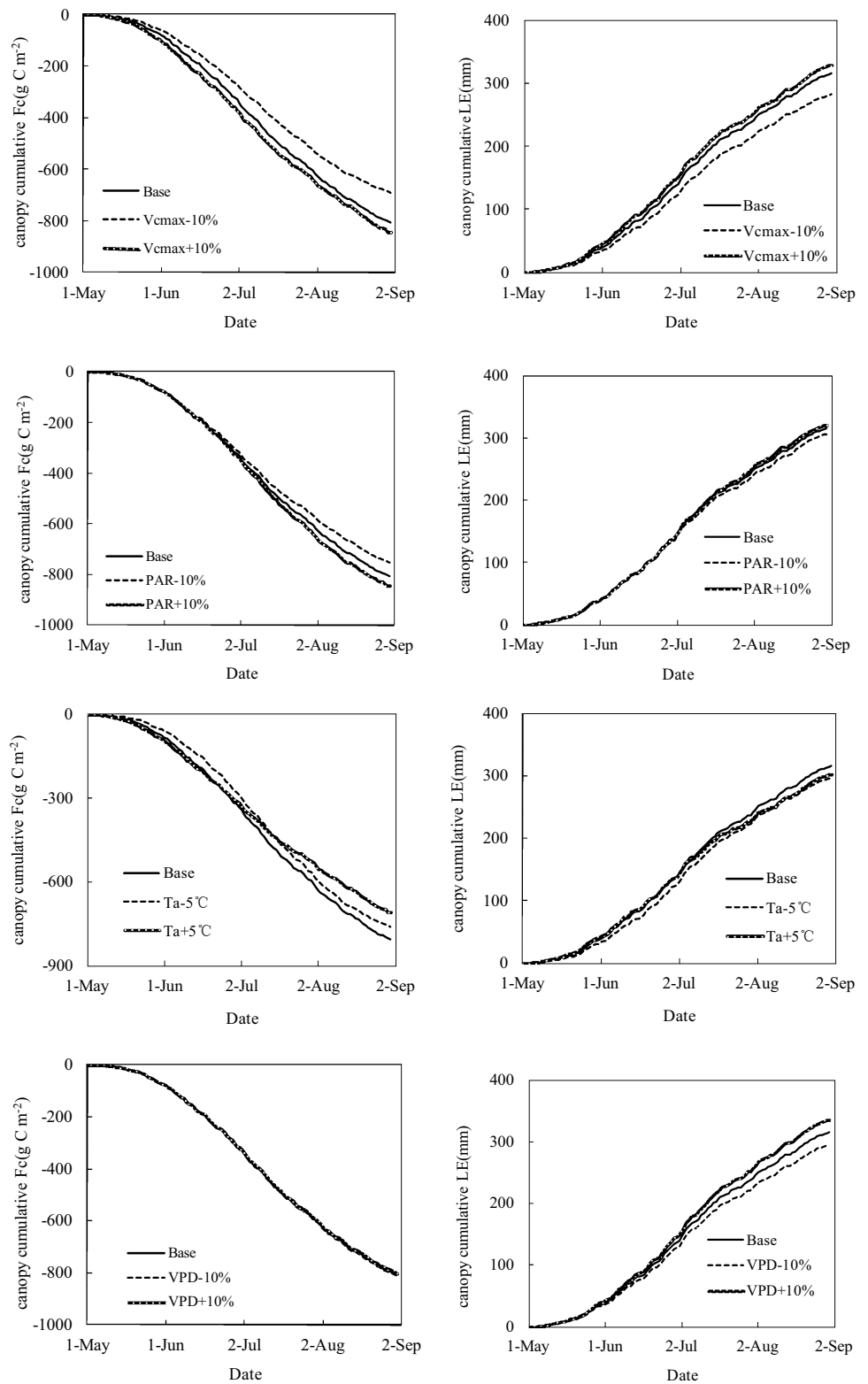
CO_2 m^{-2} s^{-1}. The parameter k_n reflects the degree of attenuation of leaf nitrogen in the canopy. The majority of leaf nitrogen is a constituent of photosynthesis-related enzymes.

The value of k_n varies among studies, and between sparse and dense canopies, with reported values ranging from 0.08 to 2.8 (Schieving et al. 1992; Archontoulis et al. 2011).

Fig. 5 (continued)
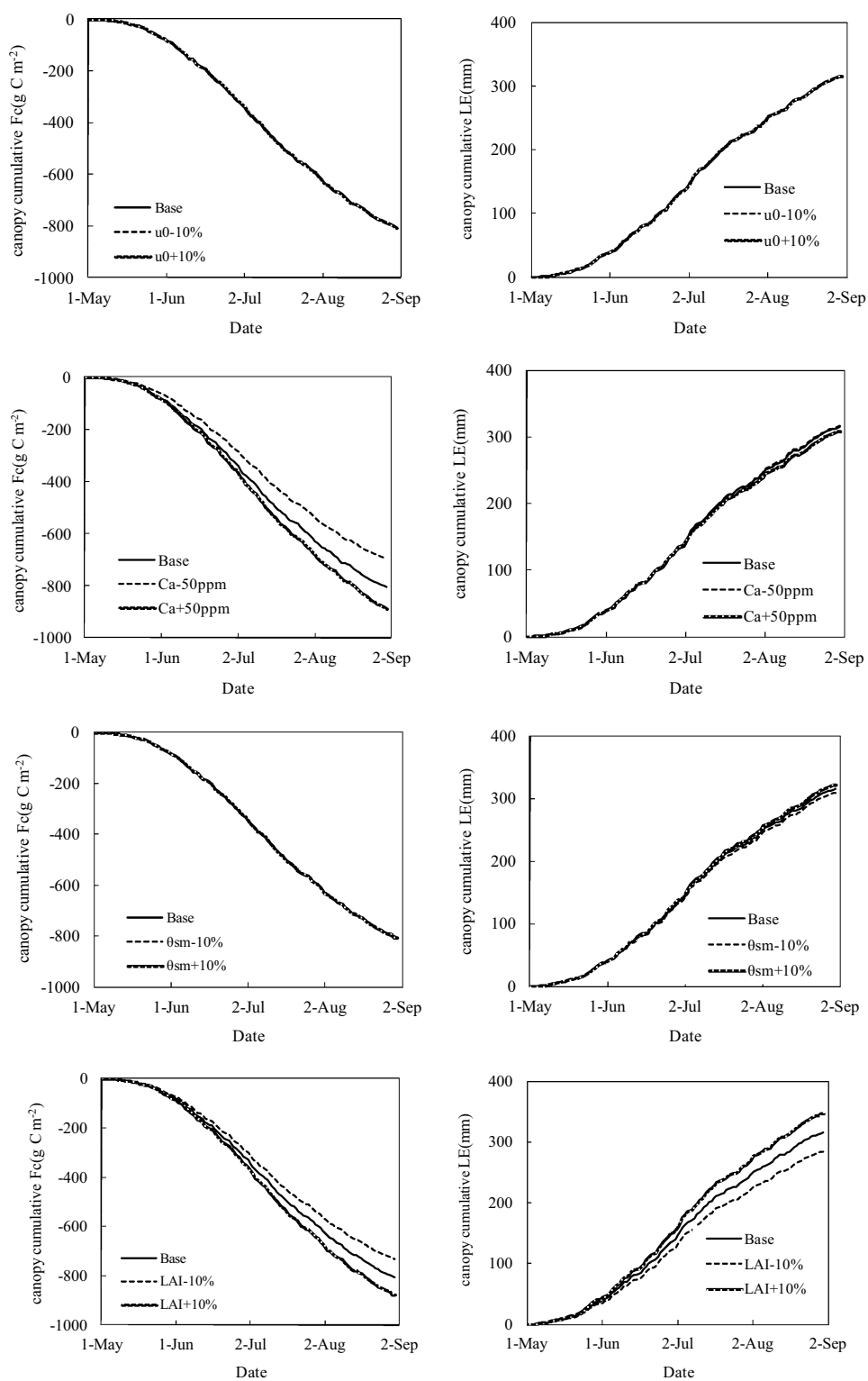
Leuning et al. (1995) showed that change in k_n (0.0–1.2) had little impact on the CO_2 assimilation rate under any light condition if the leaf nitrogen content was high. However, if the leaf nitrogen content was low, the total daily CO_2 assimilation increased by about 10–16% if k_n increased from 0.0 to 1.2. The maximum Rubisco catalytic response rate V_{cmax} varies from 23.4 to 99.6 μmol m^{-2} s^{-1} among species and observation seasons (Chen et al. 2014). In this paper, we

Table 3 Amplitude of canopy cumulative carbon and water fluxes after changes of parameters

Parameters	Parameters (initial value)	Amplitude (analysis value)	Amplitude of F_c	Amplitude of LE
Physiological parameters	$a1$ (5)	4	− 3.5%	− 14.2%
		6	+ 2.4%	+ 13.8%
	v_{pds0} (2.5)	1.5	− 3.9%	− 14.9%
		3.5	+ 1.6%	+ 8.9%
	g_{sc0} (0.03)	0.02	− 1.9%	− 10.9%
		0.04	+ 1.5%	+ 10.4%
	k_n (2.5)	2.2	+ 1.6%	+ 1.1%
		2.8	− 1.6%	− 1.2%
	V_{cmax}	+ 10%	+ 6.1%	+ 5.1%
		− 10%	− 14.8%	− 10.8%
Environmental factors	PAR	+ 10%	+ 4.5%	+ 1.3%
		− 10%	− 6.0%	− 2.6%
	T_a	+ 5 °C	− 10.7%	− 3.3%
		− 5 °C	− 6.4%	− 6.6%
	VPD	+ 10%	− 0.55%	+ 6.3%
		− 10%	+ 0.55%	− 6.5%
	u_0	+ 10%	+ 0.07%	+ 0.09%
		− 10%	− 0.06%	− 0.10%
	C_a	+ 50 µmol mol^{-1}	+ 11.0%	− 1.69%
		− 50 µmol mol^{-1}	− 13.2%	+ 0.38%
	θ_{sm}	+ 10%	+ 0.21%	+ 1.89%
		− 10%	− 0.26%	− 1.97%
Vegetation characteristic parameter	LAI	+ 10%	+ 8.9%	+ 9.8%
		− 10%	− 9.1%	− 9.9%

evaluated a1 as 5, Vpd$_{s0}$ as 1.5 kPa, g_{sc0} as 0.03 mol m^{-2} s^{-1}, k_n as 2.5, and V_{cmax} as 23.4–99.6 µmol m^{-2} s^{-1} separately among five species. We further analyzed the sensitivity of multilayered model to parameters and variables, the results indicated that F_c was more sensitive to k_n and V_{cmax}, whereas LE showed greater sensitivity to other physiological parameters (a_1, V$_{pds0}$ and g_{sc0}).

References

Amthor, J. S. (1994). Scaling CO$_2$-photosynthesis relationships from the leaf to canopy. *Photosynthesis Research, 39,* 321–350.

Aphalo, P. J., & Jarvis, P. G. (1993). The boundary layer and the apparent responses of stomatal conductance to wind speed and to the mole fractions of CO$_2$ and water vapour in the air. *Plant Cell and Environment, 16,* 771–783.

Archontoulis, S. V., Vos, J., Yin, X., Bastiaans, L., Danalatos, N. G., & Struik, P. C. (2011). Temporal dynamics of light and nitrogen vertical distributions in canopies of sunflower, kenaf and cynara. *Field Crops Research, 122,* 186–198.

Chang, K. Y., Tha, P. U. K., & Chen, S. H. (2018). The importance of carbon-nitrogen biogeochemistry on water vapor and carbon fluxes as elucidated by a multiple canopy layer higher order closure land surface model. *Agricultural and Forest Meteorology, 259,* 60–74.

Chen, N. N., Guan, D. X., Jin, C. J., Yuan, F. H., & Yang, H. (2011). Characteristics of soil respiration on horqin meadow. *Chinese Journal of Grassland, 33*(5), 82–87.

Chen, N. N., Wang, A. Z., Jin, C. J., Yuan, F. H., Wu, J. B., Guan, D. X., et al. (2014). Variability of photosynthetic parameters of five species in a temperate meadow in eastern Inner Mongolia. *Journal of Food Agriculture and Environment, 12*(2), 939–942.

Drollinger, S., Müller, M., Kobl, T., Schwab, N., Böhner, J., Schickhoff, U., et al. (2017). Decreasing nutrient concentrations in soils and trees with increasing elevation across a treelineecotone in rolwaling himal, Nepal. *Journal of Mountain Science, 14*(5), 843–858.

Farquhar, G. D., von Caemmerer, S., & Berry, J. A. (1980). A biochemical model of photosynthetic CO_2 assimilation in leaves of C_3 species. *Planta, 149,* 78–90.

Fell, M., Barber, J., Lichstein, J. W., & Ogle, K. (2018). Multidimensional trait space informed by a mechanistic model of tree growth and carbon allocation. *Ecosphere, 9*(1), e02060.

Goudriaan, J., & van Laar, H. H. (1994). *Modelling potential crop growth processes*. Dordrecht: Kluwer Academic Publishers.

Han, G. D., Hao, X. Y., Zhao, M. L., Wang, M. J., Ellert, B. H., & Walter, W. (2008). Effect of grazing intensity on carbon and nitrogen in soil and vegetation in a meadow steppe in Inner Mongolia. *Agriculture Ecosystems Environment, 125,* 21–32.

Harley, P. C., Thomas, R. B., Reynolds, J. F., & Strain, B. R. (1992). Modeling photosynthesis of cotton grown in elevated CO_2. *Plant Cell and Environment, 15,* 271–282.

He, L., Li, J., Harahap, M., & Yu, Q. (2017). Scale-specific controller of carbon and water exchanges over wheat field identified by ensemble empirical mode decomposition. *International Journal of Plant Production*. https://doi.org/10.1007/s42106-017-0005-8.

Huang, C. W., Domec, J. C., Ward, E. J., Duman, T., Manoli, G., Parolari, A. J., et al. (2016). The effect of plant water storage on water fluxes within the coupled soil-plant system. *New Phytologist, 213*(3), 1093–1106.

Huang, G., Li, Y., & Su, Y. G. (2015). Effects of increasing precipitation on soil microbial community composition and soil respiration in a temperate desert, northwestern China. *Soil Biology Biochemistry, 83,* 52–56.

IPCC. (2001). *Climate change 2001: the scientific base-contribution of working group I to the IPCC third assessment report*. New York: Cambridge University Press.

Kucharik, C. J., Barford, C. C., Maayar, M. El., Wofsy, S. C., Monson, R. K., & Baldocchi, D. D. (2006). A multiyear evaluation of a dynamic global vegetation model at three AmeriFlux forest sites: vegetation structure, phenology, soil temperature, and CO_2 and H_2O vapor exchange. *Ecological Modelling, 196,* 1–31.

Leuning, R. (1995). A critical appraisal of a combined stomatal-photosynthesis model for C_3 plants. *Plant Cell and Environment, 18,* 339–357.

Leuning, R., Dunin, F. X., & Wang, Y. P. (1998). A two-leaf model for canopy conductance, photosynthesis and partitioning of available energy: II. Comparison with measurements. *Agricultural and Forest Meteorology, 91,* 113–125.

Leuning, R., Kelliher, F. M., De Pury, D. G. G., & Schulze, E. D. (1995). Leaf nitrogen, photosynthesis, conductance and transpiration: scaling from leaves to canopies. *Plant Cell and Environment, 18*(10), 1183–1200.

Liao, G., & Jia, Y. (1996). *Grassland resource of China*. Beijing: Chinese Science and Technology Publisher.

Liu, M., He, H. L., Ren, X. L., Sun, X. M., Yu, G. R., Han, S. J., et al. (2015). The effects of constraining variables on parameter optimization in carbon and water flux modeling over different forest ecosystems. *Ecological Modelling, 303,* 30–41.

McMurtrie, R. E., Leuning, R., Thompson, W. A., & Wheeler, A. M. (1992). A model of canopy photosynthesis and water use incorporating a mechanistic formulation of leaf CO_2 exchange. *Forest Ecology and Management, 2*(1/4), 261–278.

Qu, J., & Zhao, D. (2016). Stabilising the cohesive soil with palm fibre sheath strip. *Road Materials and Pavement Design, 17*(1), 87–103.

Reed, D. E., Ewers, B. E., Pendall, E., Naithani, K. J., Kwon, H., & Kelly, R. D. (2018). Biophysical factors and canopy coupling control ecosystem water and carbon fluxes of semiarid sagebrush ecosystems. *Rangeland Ecology Management, 71,* 309–317.

Schieving, F., Pons, T. L., Werger, M. J. A., & Hirose, T. (1992). The vertical distribution of nitrogen and photosynthetic activity at different plant densities in Carex acutiformis. *Plant and Soil, 14,* 9–11.

Sellers, P. J., Berry, J. A., Collatz, G. J., Field, C. B., & Hall, F. G. (1992). Canopy reflectance, photosynthesis, and transpiration. III. A reanalysis using improved leaf models and a new canopy integration scheme. *Remote Sensing of Environment, 42*(3), 187–216.

Sellers, P. J., Randall, D. A., Collatz, G. J., Berry, J. A., Field, C. B., Dazlich, D. A., et al. (1996). A revised land surface parameterization (SiB2) for atmospheric GCMs Part I: model formulation. *Journal of Climate, 9*(4), 679–705.

Shen, X., Zhang, M. Z., & Qi, X. B. (2011). Comparison of regional forest carbon estimation methods based on regression and stochastic simulation. *Scientia Silvae Sinicae, 47*(6), 1–8.

Shi, T. T., Guan, D. X., Wang, A. Z., Wu, J. B., Yuan, F. H., Jin, C. J., et al. (2010). Modeling canopy CO_2 and H_2O exchange of a temperate mixed forest. *Journal of Geophysical Research, 115,* D17117.

Stewart, J. B., & Verma, S. B. (1992). Comparison of surface fluxes and conductances at two contrasting sites within the Fife area. *Journal of Geophysical Research, 97*(D17), 18623–18638.

Von Caemmerer, S., & Farquhar, G. D. (1981). Some relationships between the biochemistry of photosynthesis and the gas exchange of leaves. *Planta, 153,* 376–387.

Wang, Y. P., & Leuning, R. (1998). A two-leaf model for canopy conductance, photosynthesis and partitioning of available energy I: model description and comparison with a multilayered model. *Agricultural and Forest Meteorology, 91*(1/2), 89–111.

Wullschleger, S. (1993). Biochemical limitations to carbon assimilation in C3 plants-A retrospective analysis of the A/Ci curves from 109 species. *Journal of Experimental Botany, 44,* 907–920.

Xue, W., Ko, J., Werner, C., & Tenhunen, J. (2017). A spatially hierarchical integration of close-range remote sensing, leaf structure and physiology assists in diagnosing spatiotemporal dimensions of field-scale ecosystem photosynthetic productivity. *Agricultural and Forest Meteorology, 247,* 503–519.

Yu, Q., Ren, B. H., Wang, T. Y., & Sun, S. F. (1998). A simulation of diuranal variations of photosynthesis of C3, plant leaves. *Scientia Atmospherica Sinica, 22*(6), 867–880.

Zhang, L., Mao, J. F., Shi, X. Y., Ricciuto, D., He, H. L., Thornton, P., et al. (2016). Evaluation of the community land model simulated carbon and water fluxes against observations over ChinaFLUX sites. *Agricultural and Forest Meteorology, 226–227,* 174–185.

Zhao, D., Zhao, X., Khongnawang, T., Arshad, M., & Triantafilis, J. (2018). A vis-NIR spectral library to predict clay in Australian cotton growing soil. *Soil Science Society of America Journal*. https://doi.org/10.2136/sssaj2018.03.0100.